Understanding of wavenumber spectra measured by Doppler reflectometry through simulation and related estimation of wave-plasma interaction regimes

T. Happel,[1,*] T. Görler,[1] P. Hennequin,[2] C. Lechte,[3] J. Pinzón,[1,4,5] M. Bernert,[1]
G.D. Conway,[1] S. J. Freethy,[1,6] C. Honoré,[2] U. Stroth,[1,4] and the ASDEX Upgrade Team[1]

[1]*Max-Planck-Institut für Plasmaphysik, Boltzmannstr. 2, 85748 Garching, Germany*

[2]*Laboratoire de Physique des Plasmas, Ecole Polytechnique, 91128 Palaiseau, France*

[3]*IGVP, Universität Stuttgart, Pfaffenwaldring 31, 70569 Stuttgart, Germany*

[4]*Physik-Department E28, Technische Universität München,*
James-Franck-Str. 1, 85748 Garching, Germany

[5]*Laboratorio Nacional de Fusión, Association Euratom-Ciemat, Madrid, Spain*

[6]*Plasma Science and Fusion Center, Massachusetts Institute of Technology, Cambridge, Massachusetts 02139, USA*

INTRODUCTION

Fluctuation wavenumber spectra contain a variety of information about underlying linear microinstabilities and energy transfer mechanisms. In magnetic confinement fusion research, typically two-dimensional (2D) turbulence is observed due to the strong anisotropy in perpendicular and parallel directions to the magnetic field, $k_\perp \gg k_\parallel$ [1]. Nowadays, the prevailing diagnostic to measure local wavenumber spectra is Doppler reflectometry [2–18]. However, it has been pointed out that the reliability of turbulence amplitude measurements could be affected by nonlinear wave-plasma interaction processes. These processes depend the microwave polarization. In particular, for a given density gradient length, theory predicts that nonlinear effects are encountered for extraordinary mode (X-mode) polarization at lower turbulence levels than for ordinary mode (O-mode) polarization [19, 20]. These nonlinear effects can distort measurements or even render them unreliable. Although in this work only the power response is treated, also measurements of the perpendicular velocity of density fluctuations, $v_\perp$, the radial correlation length, L_r, and other derived quantities can be affected [21]. Since the diagnostic power response can be linear, nonlinear, or even saturated, it is indispensable to understand in which of these regimes the measurement is performed. In this work, a two-dimensional full-wave (2DFW) analysis has been applied to fluctuations obtained from nonlinear turbulence simulations with the gyrokinetic code GENE [22]. Full-wave simulations have been used since more than a decade to study the complex plasma-wave interactions pertaining to Doppler reflectometer measurements and can be considered as "complete" in the sense that they contain all the

physics involved in the process [23–28]. Gyrokinetic simulations are nowadays considered to be the most complete tool to simulate core plasma microturbulence in realistic geometries [22, 29–34].

This work briefly summarizes and adds information to results published in Ref. [18], where linear, nonlinear, and saturated power response regimes have been observed. First, the experiment and wavenumber spectra are shown, followed by numerical simulations, which are then interpreted in terms of the wave-plasma interaction regime estimated via a physical optics model [35].

WAVENUMBER SPECTRA IN EXPERIMENT AND SIMULATION

Wavenumber spectra in this work have been obtained by steering the incidence angle of the probing beam of the Doppler reflectometer [36]. In total, three reflectometer systems have been used, two of them in X-mode polarization and one in O-mode polarization. A wire grid polarizer serves to couple the different polarizations into the same oversized waveguide. This setup allows for the measurement of wavenumber spectra at the same toroidal, poloidal, and radial location in the plasma. The radial overlap of measurements is achieved by using the V-band range of frequencies ($f = 50 - 75$ GHz) for O-mode [37] and W-band ($f = 75 - 105$ GHz) for X-mode [5, 37].

The plasma used to study the wavenumber spectra is an L-mode plasma in upper single null (USN) configuration. The magnetic field strength on the axis is $B_t = -2.5$ T and the plasma current is $I_p = 1.0$ MA. The density and electron temperature profiles are shown in Fig. 1(a) and (b), respectively. In Fig. 1(a), the density profile is depicted, which has been obtained with Thomson scattering [38] and Lithium beam [39] diagnostics. A fit to the data points is shown as a solid line. Furthermore, the radial measurement regions of the X-mode and O-mode channels are indicated. The radial extent of the X-mode is smaller due to the magnetic field dependence of the X-mode cutoff frequency. The electron temperature profile has been measured with the electron cyclotron emission diagnostic (ECE) and is shown in (b). Since there is no ion temperature measurement available for the discharge, for the gyrokinetic simulations used later $T_i = T_e$ is assumed.

Fig. 1(c) shows the $k_\perp$-space of the Doppler reflectometer measurements. The radial extent is mostly due to the different probing beam frequencies used, while the extent in $k_\perp$-space is obtained by scanning the incidence angle of the probing beam [36]. The radial region $\rho_{\mathrm{pol}} = 0.80 - 0.85$ shows a good overlap of measurements in $k_\perp$-space, and will be used later for the evaluation of wavenumber spectra, gyrokinetic simulation and full-wave simulation. This radial region is also depicted in real space in Fig. 1(d), where the poloidal cross-section of ASDEX Upgrade is shown. Solid lines are closed flux surfaces and dashed lines are open flux surfaces.

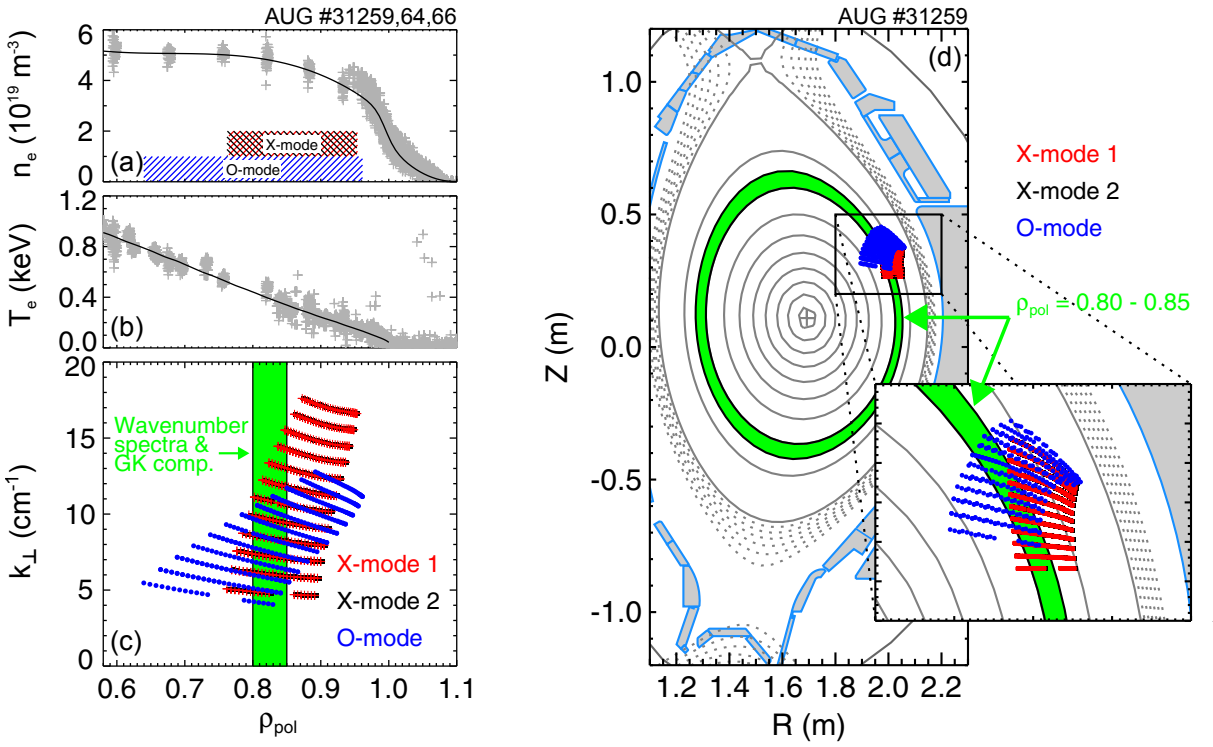

FIG. 1. Density (a) and electron temperature (b) profiles with radial measurement regions indicated for X- and O-mode. (c) Scanned wavenumber space with highlighted radial region used for further evaluation. (d) Poloidal distribution of measurements (radial region highlighted as in (c)).

Also in real space, the overlap of measurements between X-mode and O-mode is given, which makes a comparison of wavenumber spectra measured in different polarizations meaningful.

Wavenumber spectra obtained in the experiment in X- and O-mode polarization are shown in Fig. 2(a). The spectra are vertically offset to improve readability. The X-mode spectra shown in red and black have been obtained with independent reflectometer electronics. Their similarity gives confidence in the reliability of the measurement. Both spectra are rather flat in the low $k_\perp$-range up to $k_\perp \approx 9$ cm^{-1}, when a weak spectral fall-off starts with spectral indices around -3.5. In contrast, the O-mode spectrum (blue) decays already in the low $k_\perp$-range (spectral index $\alpha = -2.2$), with a transition to stronger fall-off ($\alpha = -7.2$) at higher $k_\perp$. Since the X-mode and O-mode spectra have been measured at the same position in the plasma, it is highly likely that the differences in the wavenumber spectrum shapes are due to a diagnostic effect. In the following, this difference will be reproduced by 2D full-wave simulations and an interpretation will be given using physical optics simulations [40].

The wavenumber spectra shown in Fig. 2(b) have been obtained by applying 2D full-wave simulations in X- and O-mode with the code IPF-FD3D [26] to turbulence fields generated by the gyrokinetic code GENE [22]. The nonlinear gyrokinetic simulations are flux-matched and

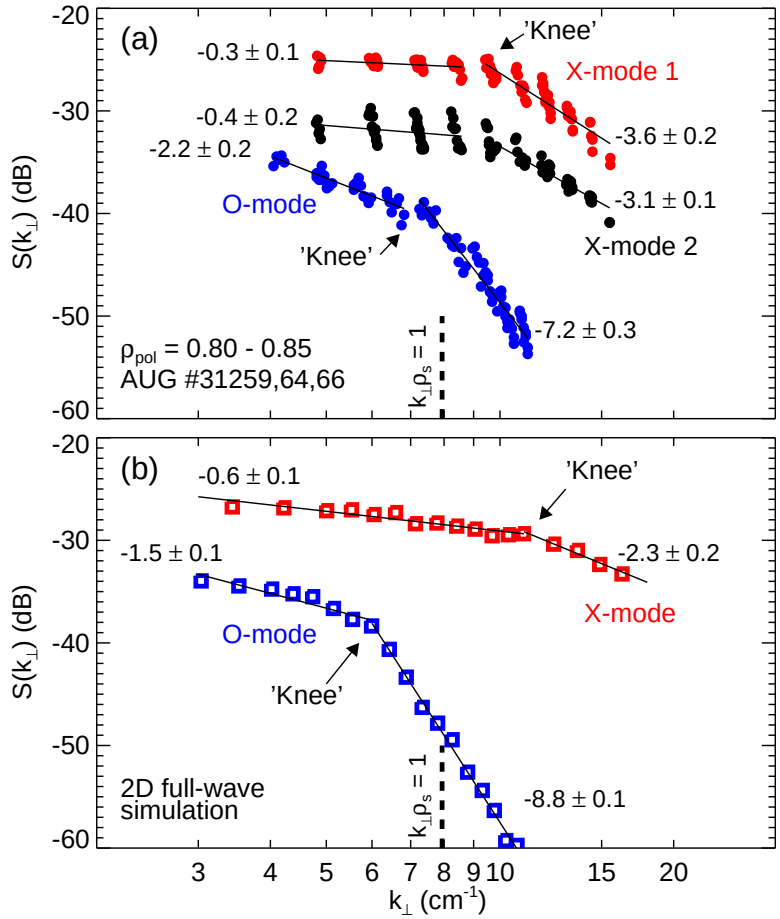

FIG. 2. Wavenumber spectra in experiment (a) and 2DFW simulation (b). The spectra are vertically offset to improve readability. X-mode (red, black) and O-mode (blue) spectra show pronounced differences, which are reproduced by 2D full-wave simulation.

the full-wave simulations have been applied to the relevant poloidal position where the Doppler reflectometry measurements have been performed [18]. As in the experimental spectra, the X-mode spectrum (red) is comparably flat at low $k_\perp$ and shows a weak spectral fall-off at high $k_\perp$. Furthermore the O-mode spectrum differs substantially from the X-mode spectrum, with a weak spectral decay at low $k_\perp$, followed by a strong spectral fall-off at high $k_\perp$. There are small differences between the spectral indices between experimental and 2DFW simulation spectra. In this context it should be noted that the 2DFW simulations require highly accurate density fluctuation levels from the gyrokinetic code while the latter is strongly sensitive to the physics inputs, i.e. requires high-accuracy profile information. Furthermore, validation of gyrokinetic codes is still an ongoing effort [41]. Considering these ongoing efforts and uncertainties in profiles, the agreement between the spectra in Fig. 2(a) and (b) is considerable.

The wavenumber spectra in Fig. 2 confirm a strong diagnostic effect when the power re-

sponse of the Doppler reflectometer is analyzed. For the same position (x, y, z) and the same turbulent background, there are differences in both the experimental spectra and the simulated spectra. This effect is due to enhanced power response and saturation, as will be shown in the next section.

ESTIMATION OF POWER RESPONSE REGIME

In order to estimate the power response regime (linear, nonlinear or saturated), the wavenumber spectrum from gyrokinetic simulation is used to generate corrugations to be analyzed with the physical optics model [20, 35]. The physical optics model is a simple and efficient model to calculate the scattering of waves off rough surfaces. For the application to the case of (Doppler) reflectometry, the rough surface corresponds to the cutoff layer which includes the turbulent fluctuations. In order to obtain the rough surface where the waves are scattered, the wavenumber spectrum from the gyrokinetic simulation is Fourier transformed with random phases to obtain a synthetic "turbulence field". This turbulence field is then translated into corrugations to be used as input for the physical optics model. For details, see Ref. [20]. In the physical optics simulations, parameter scans are done in turbulence level δn and incidence angle of the probing beam, which results in a $k_\perp$-scan. The scan in δn is represented here as a scan in the nonlinearity parameter [19]

$$\gamma = \left(\frac{\delta n}{n}\right)^2 \frac{G^2 \omega^2 x_c l_{cx}}{c^2} \ln\frac{x_c}{l_{cx}}. \tag{1}$$

Measurements are taken in the linear regime for $\gamma \ll 1$ or in the nonlinear regime for $\gamma \gg 1$. Here, $\delta n/n$ is the relative turbulence level, $\omega = 2\pi f$ is the probing wave frequency, x_c is the distance from plasma periphery to the cutoff layer, l_{cx} is the radial correlation length, and c is the speed of light in vacuum. The quantity G is the polarization-dependent enhancement factor and can be found in Ref. [42]. Values used for the evaluation of (1) are $\delta n/n = 0.9$ % and $l_{cx} = 0.031$ m (both from gyrokinetic simulation), $x_c = 0.25$ m, $f_\mathrm{O} = 64.4$ GHz (O-mode), $f_\mathrm{X} = 97.4$ GHz (X-mode), $G_\mathrm{O} = 1$ and $G_\mathrm{X} = 3.9$. Evaluation of (1) with the above parameters yields values of $\gamma_\mathrm{O} = 2.4$ (O-mode) and $\gamma_\mathrm{X} = 81.6$ (X-mode), which shows that the O-mode measurements have been performed close to the linear regime, while the X-mode measurements might have been affected by nonlinear effects.

To investigate this further, figure 3(a) shows the physical optics power response against nonlinearity parameter γ for different probing beam incidence angles, hence different $k_\perp$. The power response in the linear regime is shown as dashed lines. For $k_\perp = 0$ (perpendicular incidence), a linear regime is observed up to $\gamma \approx 2$, when the maximum in the power response is reached (saturation regime). Note that although the power response starts to saturate somewhat earlier

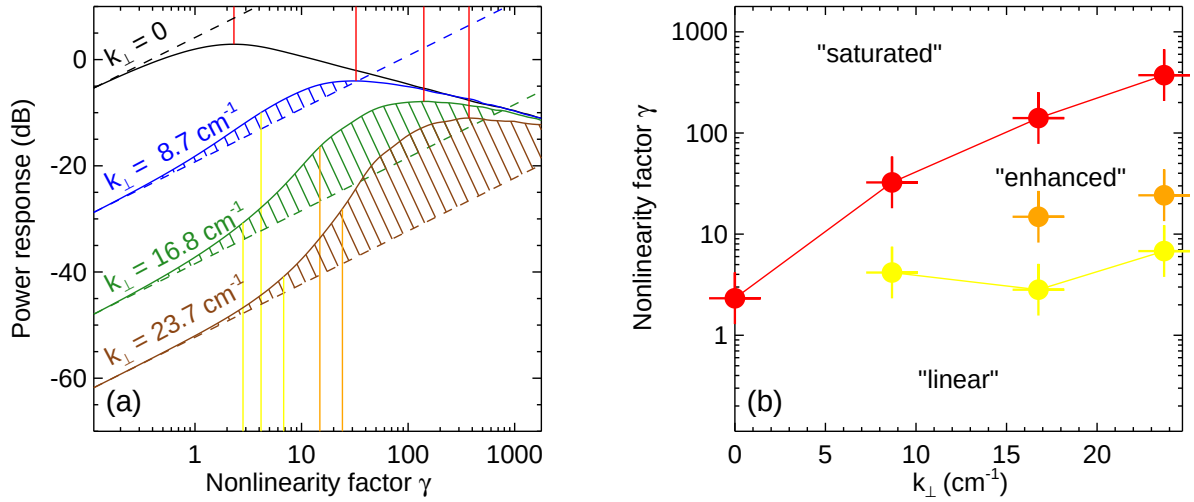

FIG. 3. (a) Physical optics power response versus nonlinearity factor γ. Both saturation and enhanced scattering regimes are found (indicated by vertical lines). (b) Saturation and enhanced power response regimes in γ-$k_\perp$-space. For details refer to the text.

($\gamma \approx 0.5$), for the sake of simplicity the response is considered linear up to the saturation value. For higher values of γ, the response to increasing γ is inverse. For higher $k_\perp$, both the linear and saturation regimes are also observed at low γ (< 1) and higher γ, respectively. However, there is a region at intermediate γ which shows an enhanced power response. This is visualized by the pattern-filled region between the expectation from a linear response (dashed line) with the simulated power response (solid line). In Fig. 3(a), the start of the saturation regime is indicated at the maximum of each curve (vertical red line) and corresponds to a respective critical value of γ. The enhanced power response regime is indicated by yellow vertical lines for an overprediction by a factor of two and orange for an overprediction by a factor of ten. Note that the γ value for the existence of both saturation and enhanced power response regimes depends on $k_\perp$, which is due to the wavenumber spectrum. An analytical extension to (1) to include the wavenumber spectrum dependence in the estimation of the enhanced power response regime has been suggested [20].

Figure 3(b) plots the critical nonlinearity factor γ of the different regimes against $k_\perp$. Above the red points, which mark the saturation detected in Fig. 3(a), the “saturation region” starts. Any measurements taken in this region will underestimate the turbulence level in the plasma. In contrast, measurements taken in the “linear region” at low γ will yield trustworthy results. The enhanced power response regime only occurs for Doppler reflectometry and not conventional reflectometry, and it will yield a measurement that overpredicts the turbulence level in the plasma.

The definitions of boundaries from Fig. 3 are applied to results from fine physical optics

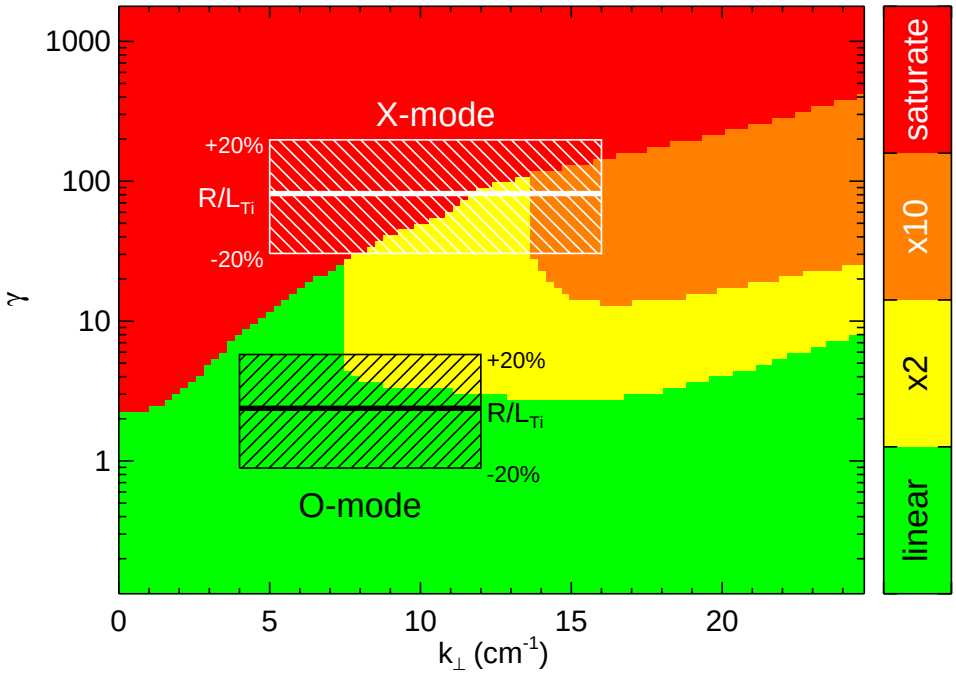

FIG. 4. Power response diagram for Doppler reflectometer measurements. Different power response regimes are identified: linear (green), enhanced (2×: yellow, 10×: orange) and saturation (red).

scans in $k_\perp$ and γ for the plasma under investigation (cf Figs. 1 and 2). The resulting existence diagram is shown in Fig. 4. Four different regions are depicted. In the linear region (green), turbulence level measurements from Doppler reflectometry are reliable and can be used to reconstruct realistic wavenumber spectra. In contrast, in the saturation region (red), turbulence measurements from Doppler reflectometry cannot be used for wavenumber studies or even for qualitative comparisons, since the power response can even be inverse (cf Fig. 3(a) at high γ values). Therefore, the calculation and interpretation of wavenumber spectra in this region is not recommended. In the enhanced power response regime (yellow and orange), a diagnostic-related flattening of wavenmber spectra at high $k_\perp$ will be observed, which hampers quantitative comparisons, e.g. with gyrokinetic codes. However, in the enhanced power response regime, qualitative statements, such as a reduction of turbulence level to changing plasma parameters, are possible.

Moreover, the parameter regimes in which the measurements in this work have been performed are indicated for both O- and X-mode in Fig. 4. Exact values are $\gamma_\mathrm{O} = 2.4$ (O-mode) and $\gamma_\mathrm{X} = 81.6$ (X-mode). Note that for the estimation of γ, the turbulence level and radial wavenumber spectrum width of the gyrokinetic simulation is used. The width in γ is determined by the turbulence level resulting from simulations with increased and decreased R/L_{Ti}. While the O-mode measurements have been taken mostly in the linear regime with possibly some enhanced power response at $k_\perp > 7$ cm^{-1}, the X-mode measurements are located in the

saturation regime at low $k_\perp$ and in the enhanced power response for $k_\perp > 12$ cm^{-1}. This effect can be seen in both the experimental and 2DFW wavenumber spectra. For X-mode, the low $k_\perp$ range is flat because the wave-plasma interaction is in the saturation regime. At high $k_\perp$, the spectral index is small, because the power response overpredicts the turbulence level (enhanced power response, cf pattern regions in Fig. 3(a)). In contrast to the X-mode, the O-mode measurements show a spectral decay in the whole range of perpendicular wavenumbers, which is consistent with $\gamma_O = 2.4$ in Fig. 4, which is located exclusively in the linear power response regime.

In summary, density wavenumber spectra have been measured with Doppler reflectometry in O- and X-mode at the same radial, poloidal and toroidal position in the ASDEX Upgrade tokamak. Not only do the measurement positions overlap in real space, there is also significant overlap in perpendicular wavenumbers. A pronounced difference is observed in spectral indices if measurements are acquired in X-mode or O-mode. Accompanying gyrokinetic simulations have been used as input to two-dimensional full-wave simulations including ASDEX Upgrade flux surface geometry. The resulting wavenumber spectra are strikingly similar to the experimental ones, which indicates that it is indeed the probing wave polarization which is responsible for the differences. Furthermore, physical optics simulations adapted to the experimental situation have been used to estimate enhanced scattering and saturation regimes. For the experimental conditions, physical optics predicts that while the O-mode measurements have been obtained in the linear regime, the X-mode measurements have been affected by both saturation and enhanced scattering regimes, depending on the probed perpendicular wavenumber. These results are consistent with the effects observed in the experimental and simulated wavenumber spectra.

The results of this paper show through experiment, simulation and comparison with theory, that wavenumber spectrum measurements via Doppler reflectometry have to be regarded with care if the nonlinearity parameter $\gamma > 1$. This criterion is reached for X-mode at lower turbulence levels than for O-mode. For quantitative analyses and comparison with gyrokinetic simulation, measurements in the linear regime are crucial. These can be more easily accessed if O-mode wave polarization is used.

This work was partly performed in the framework of the Helmholtz Virtual Institute on plasma dynamical processes and turbulence using advanced microwave diagnostics (VH-VI-526) and within the framework of the EUROfusion Consortium and has received funding from the Euratom research and training programme 2014-2018 under grant agreement No 633053. The fullwave simulations were performed on bwUniCluster funded by the Ministry of Science, Research and Arts and the Universities of the State of Baden-Württemberg, Germany, within the framework program bwHPC. The gyrokinetic simulations presented in this work were carried out using the HELIOS supercomputer system at Computational Simulation Centre of Interna-

tional Fusion Energy Research Centre (IFERC-CSC), Aomori, Japan, and at the Max Planck Computing and Data Facility (MPCDF), Garching, Germany. Furthermore, funding from the EUROfusion Enabling Research work-package AWP15-ENR-09/IPP-02 is acknowledged. The views and opinions expressed herein do not necessarily reflect those of the European Commission.

---

* Electronic address: tim.happel@ipp.mpg.de

[1] P. C. Liewer, Nucl. Fusion **25**, 543 (1985).

[2] X. L. Zou *et al.*, *Poloidal Rotation Measurement in Tore Supra by Oblique Reflectometry* (Proc. 4th International Reflectometry Workshop, Cadarache, France, 1999), report EUR-CEA-FC-1674.

[3] M. Hirsch, E. Holzhauer, J. Baldzuhn, and B. Kurzan, *Doppler Reflectometry for the Investigation of poloidally propagating Density Perturbations* (Proc. 4th International Reflectometry Workshop, Cadarache, France, 1999), report EUR-CEA-FC-1674.

[4] P. Hennequin *et al.*, Nucl. Fusion **46**, S771 (2006).

[5] C. Tröster, Ph.D. thesis, Ludwig-Maximilians-Universität München, 2008.

[6] T. Happel *et al.*, Rev. Sci. Instrum. **80**, 073502 (2009).

[7] W. A. Peebles *et al.*, Rev. Sci. Instrum. **81**, 10D902 (2010).

[8] T. Happel *et al.*, Phys. Plasmas **18**, 102302 (2011).

[9] L. Vermare *et al.*, C. R. Phys. **12**, 115 (2011).

[10] L. Vermare *et al.*, Phys. Plasmas **18**, 012306 (2011).

[11] T. Estrada *et al.*, Plasma Phys. Control. Fusion **54**, 124024 (2012).

[12] L. Schmitz *et al.*, Nucl. Fusion **52**, 023003 (2012).

[13] T. Tokuzawa *et al.*, Rev. Sci. Instrum. **83**, 10E322 (2012).

[14] F. Fernández-Marina, T. Estrada, and E. Blanco, Nucl. Fusion **54**, 072001 (2014).

[15] J. C. Hillesheim *et al.*, Nucl. Fusion **55**, 073024 (2015).

[16] U. Stroth *et al.*, Nucl. Fusion **55**, 083027 (2015).

[17] L. Schmitz *et al.*, Nat. Commun. **7**, 13860 (2016).

[18] T. Happel *et al.*, Plasma Phys. Control. Fusion **59**, 054009 (2017).

[19] E. Z. Gusakov and A. Y. Popov, Plasma Phys. Control. Fusion **46**, 1393 (2004).

[20] J. R. Pinzón *et al.*, Plasma Phys. Control. Fusion **59**, 035005 (2017).

[21] E. Z. Gusakov, A. V. Surkov, and A. Y. Popov, Plasma Phys. Control. Fusion **47**, 959 (2005).

[22] F. Jenko, W. Dorland, M. Kotschenreuther, and B. N. Rogers, Phys. Plasmas **7**, 1904 (2000).

[23] F. da Silva *et al.*, Rev. Sci. Instrum. **75**, 3816 (2004).

[24] E. Blanco, T. Estrada, and J. Sánchez, Plasma Phys. Control. Fusion **48**, 699 (2006).

[25] E. Blanco and T. Estrada, Plasma Phys. Control. Fusion **50**, 095011 (2008).

[26] C. Lechte, IEEE Trans. Plasma Sci. **37**, 1099 (2009).

[27] F. da Silva, S. Heuraux, E. Z. Gusakov, and A. Popov, IEEE Trans. Plasma Sci. **38**, 2144 (2010).

[28] J. C. Hillesheim *et al.*, Rev. Sci. Instrum. **83**, 10E331 (2012).

[29] M. Kotschenreuther, G. Rewoldt, and W. Tang, Comput. Phys. Commun. **88**, 128 (1995).

[30] A. Peeters *et al.*, Comput. Phys. Commun. **180**, 2650 (2009).

[31] J. Candy and R. Waltz, J. Comput. Phys. **186**, 545 (2003).

[32] V. Grandgirard *et al.*, Commun. Nonlinear Sci. Numer. Simul. **13**, 81 (2008).

[33] T.-H. Watanabe and H. Sugama, Nucl. Fusion **46**, 24 (2006).

[34] M. Nunami, T.-H. Watanabe, and H. Sugama, Plasma Fus. Res. **5**, 016 (2010).

[35] G. D. Conway, Plasma Phys. Control. Fusion **41**, 65 (1999).

[36] T. Happel *et al.*, *The optimized steerable W-band Doppler reflectometer on ASDEX Upgrade: possibilities and issues* (Proc. 11th International Reflectometry Workshop, Palaiseau, France, 2013).

[37] R. Sabot, P. Hennequin, and L. Colas, Fusion Sci. Technol. **56**, 1253 (2009).

[38] B. Kurzan and H. D. Murmann, Rev. Sci. Instrum. **82**, 103501 (2011).

[39] M. Willensdorfer *et al.*, Rev. Sci. Instrum. **83**, 023501 (2012).

[40] J. Pinzón *et al.*, *Power response in Doppler reflectometry* (Proc. 13th International Reflectometry Workshop, Daejeon, South Korea, 2017).

[41] A. E. White and T. Görler, Plasma Phys. Control. Fusion **59**, 050101 (2017).

[42] E. Z. Gusakov, M. A. Irzak, A. Y. Popov, and N. V. Teplova, Plasma Phys. Control. Fusion **57**, 075009 (2015).